

## Antimicrobial activity from polymeric composites-based polydimethylsiloxane/TiO<sub>2</sub>/GO: evaluation of filler synthesis and surface morphology

Camila F. Correa<sup>1</sup> · Luiza R. Santana<sup>1</sup> · Ricardo M. Silva<sup>1</sup> · Bruno S. NoreMBERG<sup>1</sup> · Rafael G. Lund<sup>2</sup> · Juliana S. Ribeiro<sup>2</sup> · Fabiana V. Motta<sup>3</sup> · Mauricio R. D. Bomio<sup>3</sup> · Rubens M. Nascimento<sup>3</sup> · Neftali L. V. Carreño<sup>1</sup>

Received: 13 May 2016/Revised: 12 August 2016/Accepted: 25 October 2016  
© Springer-Verlag Berlin Heidelberg 2016

**Abstract** Antimicrobial substances may be used to reduce hospital infections and inhibit food contamination, thus ensuring the safety and well being of humans. The objective of this study was to evaluate the antimicrobial activity of the polymeric nanocomposites polydimethylsiloxane (PDMS) embedded with two types of fillers based on titanium dioxide (commercial TiO<sub>2</sub> P25 versus TiO<sub>2</sub> via facile Microwave-assisted hydrothermal-MAH synthesis) and graphene oxide (GO). The nanocomposites were prepared using different compositions, concentrations, and functionalizations (PDMS/TiO<sub>2</sub>/GO; PDMS/TiO<sub>2</sub> and PDMS/GO). The antimicrobial activity of the samples was evaluated for different treatments on *Candida albicans*, *Staphylococcus aureus*, and *Enterococcus faecalis*, by a modified direct contact test (mDCT). The samples were also evaluated on surface morphology and the roughness as a function of active particles insertion by atomic force microscopy (AFM). Most of the PDMS films whose polymer was embedded with GO and hydrothermal TiO<sub>2</sub> showed the highest inhibition growth of bacteria and *Candida* over 24 h. After 24 h, F, J, and H samples showed the best antibacterial activity, whereas E showed the best antifungal activity. The results indicated that the nanocomposites PDMS/GO/TiO<sub>2</sub>MAH and PDMS/GO sample enhanced antimicrobial activity in the treatments tested, therefore they were functional for contaminant reduction.

---

✉ Neftali L. V. Carreño  
neftali@ufpel.edu.br

<sup>1</sup> Graduate Program Science and Materials Engineering, Technology Development Center, Federal University of Pelotas, Pelotas, RS CEP 96010-610, Brazil

<sup>2</sup> Graduate Program in Dentistry, Federal University of Pelotas, Rua Gonçalves Chaves 457, Pelotas, RS 96015-560, Brazil

<sup>3</sup> Department of Materials Engineering, Technology Center, Federal University of Rio Grande do Norte, Natal, RN CEP 59078-970, Brazil

**Keywords** Antimicrobial activity · Graphene oxide · Titanium dioxide · Polymer composite

## Introduction

The necessity for developing nanocomposites using different combinations of materials has been growing, once bacterial resistance antimicrobial materials, as it is already known, is a global problem of magnitude [1]. Treatment of infectious diseases has become increasingly sensitive, particularly in hospitalized patients [2]. Furthermore, materials with antimicrobial activity are also being used in medical devices and food packaging, to avoid bacterial contamination [2].

The polydimethylsiloxane (PDMS) is a polymer which has been highlighted as a basis for the incorporation of other materials; in addition it presents biocompatibility, stability, and biomedical antifouling properties [3, 4]. A material from carbon that has been intensively studied over the years, and applied to several areas, is graphene oxide (GO). It has great bacterial contamination potential when functionalized and attached to the PDMS polymer with silver nanoparticles (Ag), glimpsing load antibiotics, and removing bacteria [5]. Another material, which has already been diffused is titanium dioxide (TiO<sub>2</sub>), known for its important environmental applications due to its chemical stability, low cost, and photocatalytic activity when used for antibacterial action [6, 7].

Thus, the objective of this study was to develop nanocomposites based on PDMS/TiO<sub>2</sub>/GO varying concentrations, chemical routes (conventional versus Microwave-assisted hydrothermal of TiO<sub>2</sub> ultrafine particles), and combinations to evaluate their antimicrobial activity in their use in locations susceptible to contamination.

## Materials and methods

All reagents used were of analytical grade and without any further purification.

### Preparation of graphene oxide (GO)

The modified method of Hummer and Offemann [8] was used to obtain the GO, wherein 1 g of graphite powder (Cn) (Synth) was weighed and dissolved in 23 mL of sulfuric acid (H<sub>2</sub>SO<sub>4</sub>) (PA Proton Chemical) being stirred and cooled to 0 °C, using an ice bath. After 10 min, it was added to 0.5 g of sodium nitrate (NaNO<sub>3</sub>) (Synth) and 3 g of potassium permanganate (KMnO<sub>4</sub>) (Synth). During this step, the speed by which the reagents were added was carefully adjusted to maintain the temperature below 20 °C. Therefore, the ice bath was stirred for 30 min at ~24 °C. It was then added to 46 mL of deionized water and it was left under stirring for 15 min, raising its temperature to 90 °C. Finally, it was added 140 mL of distilled water and 10 mL of hydrogen peroxide solution (H<sub>2</sub>O<sub>2</sub>) (Synth, 29% content). The

solid was then separated from the solution by centrifugation, at a speed of 6.000 rpm for 5 min, and washed several times with deionized water. Then the solid was dried in an oven without air circulation at 50 °C for 72 h. Finally, the dried powder was ground in a mortar to become a fine powder.

### Preparation of PDMS matrix

The preparation of PDMS (Sylgard 184, Dow Corning) was carried out according to the manufacturer's information of 10:1 ratio, in which 30 g of the mixture basic (dimethyl-siloxane-dimethyl-vinyl-terminated) was combined with 3 g of the curing agent (methylhydrogen-dimethyl-siloxane). The solution was manually mixed with a glass rod, until obtaining a homogeneous system. After mixing, 3 g of the PDMS mixture was poured onto different Petri dishes, which were kept standing at 24 °C to remove the oxygen bubbles.

### TiO<sub>2</sub> prepared via Microwave-assisted hydrothermal method

The TiO<sub>2</sub> obtained by Microwave-assisted hydrothermal synthesis was based on the literature with some modifications [9], where 0.30 g of previously prepared titanium glycolate was dispersed in 50 mL absolute ethanol (Synth) using cutting-edge ultrasound (Unique, Brazil) for 20 min at 40 Hz. Then 50 mL of distilled water was added to the solution and sonicated for 2 min. The final dispersion was placed in a polytetrafluoroethylene (PTFE) vessel and heated at 150 °C for 20 min. Afterwards, it was cooled to room temperature at ~24 °C. Then, the white precipitate was collected and washed three times with absolute ethyl alcohol. The precipitate was washed and dried (A5SE, DeLeo, Brazil) in an oven with no air flow for 12 h and stored for further characterization (herein after referred to as the material is TiO<sub>2</sub>-MAH).

### Preparation of solutions and samples

The solutions containing the particles to be incorporated in the PDMS were prepared with 8 mg (100%), 6 mg (75%), 4 mg (50%), and 3 mg (25%) of GO, mixed with different types of TiO<sub>2</sub>, prepared via MAH (TiO<sub>2</sub>-MAH) and commercially TiO<sub>2</sub> (referred as TiO<sub>2</sub> P25, from Evonik Brazil). The particles were dispersed in 10 mL of absolute ethanol (Synth) using ultrasound (UNIQUE, 30 Hz, 1000 W) for 5 min. Table 1 shows the composition and concentrations of each sample, identified with letters, which were prepared based on a preliminary study.

The samples were prepared by two methods, by dripping solutions on the surface of the film (Fig. 1a) and through manual mixing of solutions in the uncured PDMS as shown in Fig. 1b.

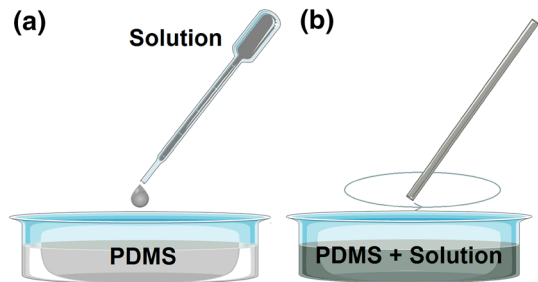
### Characterizations

The X-Ray analysis (XRD) was used to obtain the materials' structural characteristics and it was possible to determine the crystalline phases formed in

**Table 1** Description of samples

Treatments	% wt GO	% wt TiO <sub>2</sub> P25	% wt TiO <sub>2</sub> -MAH
A	50	50	–
B	–	100	–
C	–	–	100
D	25	–	75
E	50	–	50
F	75	–	25
G	25	75	–
H	100	–	–
I	75	25	–
J	–	–	–

**Fig. 1** **a** Samples prepared by the by dripping on PDMS; **b** Samples prepared by homogenization of the solution in PDMS



the synthesis process. The XRD patterns were obtained on a Shimadzu diffractometer, Model XRD-6000, employing the powder method, using scan angles of 10° to 80°.

A field-emission scanning electron microscope (FESEM; JSM-7500F, JEOL, Japan) was used to evaluate the morphology of the TiO<sub>2</sub>-MAH sample.

The determination of the surface area of the nanoparticles was obtained using the multimolecular adsorption theory, together with measurements of physical adsorption of N<sub>2</sub> gas. This was carried out at a temperature of –196 °C by the method of brunauer-emmett-teller (BET). The adsorption and desorption isotherms aimed at determining the specific surface area ( $S_{\text{BET}}$ ) of the material. Measurements were obtained on a surface area analyzer (BELSORP-mini, BEL Japan, Japan). 0.246 g of each sample was weighed and subsequently dried at 120 °C, under a stream of N<sub>2</sub> for 3 h.

AFM analysis allows the surface of a sample to be monitored with a probe, to provide the surface topography. The analysis was performed using an atomic force microscope (AFM, SPM-9700, Shimadzu, Japan) in no-contact mode with a 1.0 Hz scan speed. Static water contact angles (CAs) of the nanocomposite surfaces were measured with a contact angle meter (AttensionTheta, Biolin Scientific), based on a sessile drop measuring method, with a water drop volume of 5 μL.

## Antibacterial activity

The evaluation of the antimicrobial effect was performed by the modified direct contact test. The modified direct contact test consists of the measurement of cinematic microbial growth, by close contact between the micro-organism tested and the material [10], using microplate 96-well cell cultures. Previous to the test, the samples were sterilized by UV (ultraviolet) light inside a laminar flow chamber. After the sterilization of the specimens, they were placed in 96 well plates, with  $n = 6$  for each group tested.

## Bacterial strains and culture conditions

*Escherichia coli* ATCC29214, *Candida albicans* ATCC62343, and *Staphylococcus aureus* ATCC19095 were selected because they are pathogens frequently present in hospital infections [11, 12] and food contamination [13]. The selected bacteria were individually grown overnight on Tryptic Soy Agar (TSA) plates (*E. coli* and *S. aureus*), and on Sabouraud Dextrose Agar (SDA) plates (*C. albicans*) in aerobic conditions, at 37 °C for 24 h. Colonies of microorganisms were then suspended separately in Tryptic Soy Broth (TSB) for *E. coli* and *S. aureus*, and Sabouraud Dextrose Agar for *C. albicans*, to make suspensions of  $3 \times 10^8$  CFU/mL, the microbial cell turbidity was adjusted using spectrophotometry (spectrophotometer, Quimis, Brazil) at 405 nm. From this inoculum, 20  $\mu$ L of bacterial suspension was added into each well, to then be evaluated.

## Modified direct contact test (mDCT)

The materials were placed in the microplate wells  $n = 6$ , with the aid of sterile forceps. A specimen will be present in each well and the material was then inoculated with 20  $\mu$ L of microbial suspension (*C. albicans* + Sabouraud broth, *E. coli* and *S. aureus* + TSB). The disks were incubated for 1 and 24 h at 37 °C and approximately 100% of relative humidity. Microplate wells containing the same volume of bacterial suspension without test disks were also incubated as controls.

After, 180  $\mu$ L of culture medium supplemented with 10% sucrose (Tryptic Soy Broth—TSB for *E. coli* and *S. aureus* and Sabouraud Dextrose Agar—SDA for *C. albicans*) was added in each well and shaken (Guangzhou Mekan Trading Co., Ltd., China) for 10 min. One hundred microliters of the bacterial suspension from each well was transferred for dilution. Serial dilutions and plating were carried out in disposable Petri dishes containing SDA for *C. albicans* and TSA for *E. coli* and *S. aureus*, divided into eight parts. Each plate received two drops of 20  $\mu$ L per dilution. The plates were then incubated at 37 °C for 24 h. Beyond the period of incubation, the Colony Forming Units (CFU/mL) [11] were counted.

Three independent experiments were performed in triplicate. Thus, a total of nine disks from each group were used for each bacterium at each time point

For microbiological activity, data were analyzed using a *t* test, an ANOVA, and complementary test Student–Newman–Keuls for multiple comparisons.  $\alpha = 5\%$  was considered for all statistical analyzes. Data are expressed in mean  $\pm$  SEM.

## Results and discussions

### Characterization analysis of polymer composites

The diffraction patterns of X-rays of conventional  $\text{TiO}_2$  P25 and  $\text{TiO}_2$ -MAH are shown in Fig. 2a. All diffraction peaks relating to the  $\text{TiO}_2$ -MAH sample can be indexed to a structure of anatase type according to the standard JCPDS No. 21-1272:  $25.22^\circ$  (101);  $37.81^\circ$  (004);  $47.95^\circ$  (200);  $54.39^\circ$  (105);  $62.69^\circ$  (204). For the sample  $\text{TiO}_2$  P25, the diffraction pattern showed, as expected, a peak also referring to the rutile phase at  $27.4^\circ$  (110). The intensities of the peaks related to the  $\text{TiO}_2$ -MAH sample showed more extensive and lower intensities, indicating a lower crystallinity and hence smaller particle size. In the inserted pattern in Fig. 2a, it was observed that the characteristics of graphite diffraction peaks at (002) and (004) in GO were displaced to  $10, 24^\circ$  and  $42, 58^\circ$ , respectively, as a result of exfoliation of graphite layers [14]. Table 2 shows the pore size distribution characteristics between the MAH- $\text{TiO}_2$  and  $\text{TiO}_2$  nanoparticles conventional P25 isotherms obtained by nitrogen adsorption measurements. It can be shown that the surface area of the  $\text{TiO}_2$ -MAH sample showed a value of  $145.15 \text{ m}^2\text{g}^{-1}$ , i.e., which is relatively high compared with the value of  $44.968 \text{ m}^2\text{g}^{-1}$ , regarding the sample  $\text{TiO}_2$  P25 [15].

AFM analysis illustrates the morphological characteristics of the materials and the effect of different particle insertions on the surface. The roughness results are expressed in Fig. 3 and Table 3. An increase in roughness was noticed by preparing particles dropped directly (casting) on the surface of the polymer compared to the homogeneous solution prepared, with the exception for GO particles. This might have occurred because the nanoparticles remain in larger amounts on the sample surface. The roughness values obtained for sample 3.1c were higher than those obtained for sample 3.1d. This is because the  $\text{TiO}_2$  nanoparticles via MAH have high surface area and therefore the agglomeration of these nanoparticles occurs. The results for the GO samples showed a lower roughness value. The PDMS AFM images are equivalent to the PDMS views in literature [5]. Analyzing the

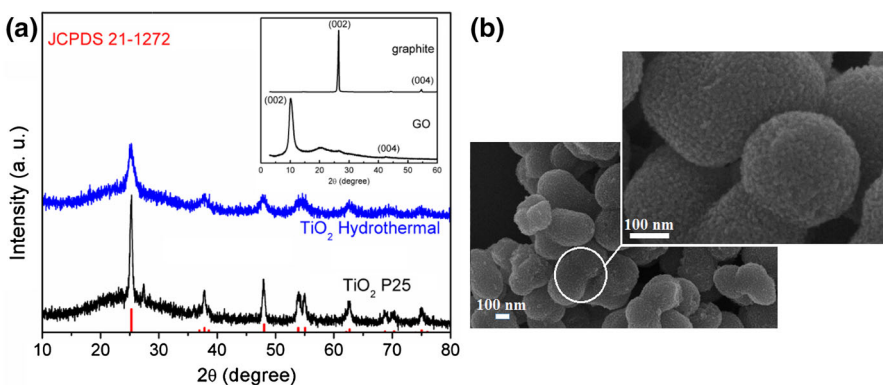


**Fig. 2** a Diffratogram in comparison to JCPDS No. 21-1272 referred the structure of anatase type titanium dioxide. With insertion of Graphite and GO patterns b FESEM images of  $\text{TiO}_2$ -MHA

**Table 2** BET data of nanoparticles

Sample	TiO <sub>2</sub> -MAH	P25 TiO <sub>2</sub>
BET superficial area (m <sup>2</sup> g <sup>-1</sup> )	145.15	44.968
Total volume of pores (cm <sup>3</sup> g <sup>-1</sup> ) <sup>a</sup>	0.2689	0.0573
Pore diameter (nm) <sup>b</sup>	7.4112	5.1012

<sup>a</sup> Total pore volume of pores of a single point in P/P0, 0.95

<sup>b</sup> BJH desorption average pore diameter

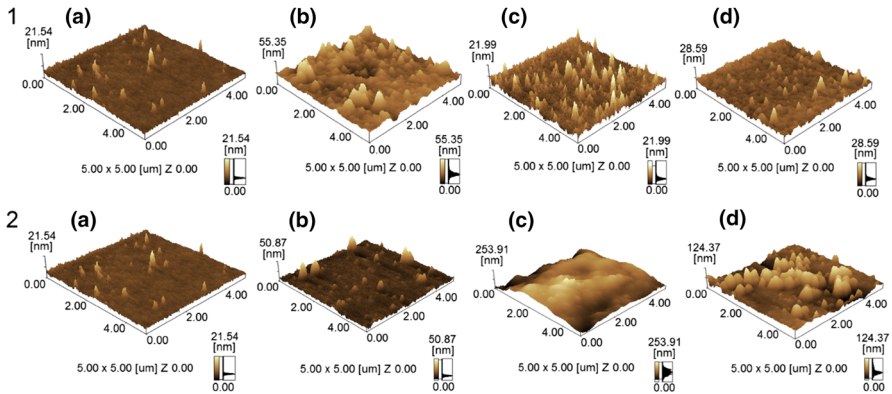


**Fig. 3** AFM images of (1) homogeneous solution and (2) particles dropped direct (casting) on the polymer surface of: **a** PDMS; **b** PDMS/GO; **c** PDMS/GO/TiO<sub>2</sub>MAH; and **d** PDMS/GO/TiO<sub>2</sub>-P25, respectively

**Table 3** Roughness (Z) of sample films by casting and homogeneous method

PDMS composite by homogeneous solution	CA (nm)	PDMS composite by particles casting direct on the polymer surface	Z (nm)
a) Sample J	21.54	a) Sample J	21.54
b) Sample H	55.35	b) Sample H	50.87
c) Sample E	21.99	c) Sample E	253.91
d) Sample I	28.59	d) Sample I	124.37

results of Table 3, it is possible to note that the direct dropping method on the surface produces a rougher surface compared to the homogeneous solution method. Consequently, the higher the roughness the greater the surface area will be. This explains why the samples prepared by the drip method showed a better antimicrobial response. In fact, the effect could also be better because this method maintains a higher concentration of particles on the surface (where the effect occurs).

The light and dark regions displayed in some samples can be identified as hydrophobic and hydrophilic domains, respectively. The same examples are reported on literature [16, 17].

As shown in Table 4, the angle value of the water contact of the PDMS composite by homogeneous solution and the composite by the particles casting direct on the polymer surface reaches 115.5 and 102.4, respectively. By transferring the GO and TiO<sub>2</sub> particles onto the surface of PMDS substrate, the static water contact angle for all samples decreased. Noticeably, the difference in the interaction of the composites by the homogeneous solution of the films with the incorporation of the particles (casting method) on the polymer surface occurs due to a monolayer formation. Thus, the interactions of oxide surface (strongly hydrophilic) and PDMS (hydrophobic) with water strongly differ. Therefore, interactions of the samples H, E, and I PDMS composites by the particle casting direct on the polymers surface with water. The nanoscale shows the hydrophilicity of composites with respect to water due to the hydrophilic character of TiO<sub>2</sub> and GO materials.

### Antimicrobial activity on films surface

The Direct Contact Test was first introduced by Weiss et al. [18] to evaluate the antimicrobial effect of endodontic sealers and root-end filling materials. This methodology was based on measuring the effect of close contact between test bacteria and the tested material, on the kinetics of the bacterial outgrowth. It is a turbidimetric method to detect bacterial growth. However, there may be cases where there is turbidity, but the bacterium dies. Therefore, the method chosen was the MDCT because of the modification described by Zang et al. [10]. In this study, the plating was done immediately after each time of contact (time-point). This modification makes it possible to measure the bactericidal effect rather than the bacteriostatic effect of the materials tested. Moreover, it is possible to calculate the exact number of surviving and viable bacteria by counting the colony forming units [10].

The results of the antimicrobial activity of PDMS films prepared by two steps (Table 5) showed that for *S. aureus* and *E. coli*, the growth was lower, especially for the H group (which had the best results). In the test for the fungus *Candida*, the H group had better results. In the case of the three bacteria, groups A and G were the worst, promoting a high bacterial growth ( $P < 0.05$ ) compared with controls, both among groups and between 1 and 24 h.

After the preliminary tests, an assessment of antibacterial activity of the films prepared in one step of *Candida albicans*, *Staphylococcus aureus*, and *Enterococcus faecalis* by a modified direct contact test (mDCT), shown in Table 6.

**Table 4** Contact angle of films sample by casting and homogeneous method

PDMS composite by homogeneous solution	CA (degree)	PDMS composite by particles casting direct on the polymer surface	CA (degree)
a) Sample J	99.9	a) Sample J	99.9
b) Sample H	98.5	b) Sample H	87.1
c) Sample E	102.5	c) Sample E	90.5
d) Sample I	105.5	d) Sample I	102.4

**Table 5** Preliminary tests of antimicrobial activity to PDMS/GO/TiO<sub>2</sub> films to *S. aureus*, *E. coli* and *C. albicans*

Films	<i>S. aureus</i>		<i>E. coli</i>		<i>C. albicans</i>	
	1 h	24 h	1 h	24 h	1 h	24 h
A	11.32 ± 0.16A <sup>a</sup>	11.43 ± 0.23B <sup>b</sup>	10.75 ± 0.15A <sup>a</sup>	11.32 ± 0.16B <sup>a</sup>	10.8 ± 0.07A <sup>a</sup>	10.79 ± 0.05A <sup>a</sup>
B	9.79 ± 0.53A <sup>b</sup>	9.86 ± 0.50A <sup>c</sup>	9.81 ± 0.51A <sup>b</sup>	9.69 ± 0.97A <sup>b</sup>	9.44 ± 0.58A <sup>b</sup>	9.34 ± 0.49A <sup>b</sup>
C	10.19 ± 0.14A <sup>b</sup>	9.91 ± 0.26A <sup>c</sup>	10.37 ± 0.02A <sup>b</sup>	10.42 ± 0.91A <sup>c</sup>	10.31 ± 0.06A <sup>b</sup>	10.29 ± 0.10A <sup>b</sup>
D	9.59 ± 0.69A <sup>b</sup>	10.15 ± 0.41B <sup>c</sup>	9.88 ± 0.54A <sup>b</sup>	10.23 ± 0.10A <sup>b</sup>	10.13 ± 0.56A <sup>b</sup>	9.69 ± 0.54A <sup>b</sup>
E	8.23 ± 0.25A <sup>b</sup>	8.19 ± 0.24A <sup>c</sup>	8.07 ± 0.16A <sup>c</sup>	8.41 ± 0.71A <sup>b</sup>	8.19 ± 0.02A <sup>b</sup>	7.97 ± 0.16A <sup>b</sup>
F	8.17 ± 0.67A <sup>b</sup>	7.82 ± 0.44A <sup>c</sup>	8.13 ± 0.51A <sup>c</sup>	8.29 ± 0.81A <sup>b</sup>	7.97 ± 0.5A <sup>c</sup>	7.77 ± 0.51A <sup>b</sup>
G	11.36 ± 0.28A <sup>a</sup>	10.82 ± 0.16B <sup>d</sup>	11.08 ± 0.04A <sup>d</sup>	11.36 ± 0.97B <sup>a</sup>	11.19 ± 0.01A <sup>c</sup>	11.00 ± 0.04A <sup>c</sup>
H	6.93 ± 0.49A <sup>b</sup>	6.78 ± 0.49A <sup>c</sup>	6.78 ± 0.50A <sup>c</sup>	6.9 ± 0.75A <sup>b</sup>	7.11 ± 0.53A <sup>b</sup>	6.77 ± 0.5A <sup>b</sup>
I (control samples)	8.38 ± 1.16A <sup>b</sup>	8.81 ± 1.38A <sup>c</sup>	8.61 ± 1.40A <sup>c</sup>	8.57 ± 0.06A <sup>b</sup>	8.22 ± 1.35A <sup>b</sup>	9.07 ± 1.4A <sup>b</sup>
J (bacterial control)	7.25 ± 0.51A <sup>b</sup>	7.13 ± 0.54A <sup>c</sup>	6.84 ± 0.54A <sup>c</sup>	7.05 ± 0.25A <sup>b</sup>	6.51 ± 0.53A <sup>b</sup>	6.82 ± 0.42A <sup>b</sup>
K	7.05 ± 0.43A <sup>b</sup>	6.77 ± 0.11A <sup>c</sup>	7.1 ± 0.54A <sup>c</sup>	7.25 ± 0.46A <sup>b</sup>	7.08 ± 0.51A <sup>b</sup>	7.14 ± 0.37A <sup>b</sup>

Different lowercase letters in the same column represent a statistically significant difference among the groups at same exposure time ( $P < 0.05$ ). Different capital letters indicate the differences of each group at both different exposure times (1 and 24 h) ( $P < 0.05$ )

Different superscript letters represent statistically significant differences between groups and exposure times

**Codes:** **A:** PDMS film by casting and homogeneous method with 50% wt GO and 50%wt TiO<sub>2</sub>; **P25;** **B:** PDMS film by casting and homogeneous method with 100% wt TiO<sub>2</sub>; **P25;** **C:** PDMS film by casting and homogeneous method with 100% wt TiO<sub>2</sub> prepared by MAH method; **D:** PDMS film by casting and homogeneous method with 25% wt GO and 75% wt TiO<sub>2</sub> prepared by MAH method; **E:** PDMS film by casting and homogeneous method with 50% wt GO and 50% wt TiO<sub>2</sub> prepared by MAH method; **F:** PDMS film by casting and homogeneous method with 75% wt TiO<sub>2</sub> prepared by MAH method; **G:** PDMS film by casting and homogeneous method with 25% wt GO and 75% wt TiO<sub>2</sub>; **P25;** **H:** PDMS film by casting and homogeneous method with 100% wt GO; **I:** PDMS film by casting and homogeneous method with 75% wt GO and 25% TiO<sub>2</sub>; **P25;** and **J:** PDMS film

The maximum antibacterial activity observed for *C. albicans* in 1 h was in group H. In 24 h, E was the group that had the highest antifungal activity. The antibacterial activity of all samples was less than 1 h exposure, statistically significant differences were observed between both time periods ( $P < 0.05$ ). The group E was the only that improve the antifungal activity in 24 h showing the highest antifungal activity in 24 h.

For *S. aureus* in the first hour, the group E had significantly lower antibacterial activity when compared to the other groups ( $P < 0.05$ ). Statistically, the other groups had similar results, with a lower performance since they had higher bacterial growth. In 24 h, F, J and H showed the highest antibacterial activity.

The nanocomposites with TiO<sub>2</sub> demonstrate that films have improved barrier properties, such as films reported in the literature [19, 20]. For *E. coli* in hour 1, when comparing the groups, it was observed that group E showed less bacterial growth and increased antimicrobial activity. Already the groups F and H had statistically similar results whereas the groups J and I had higher bacterial growth.

Within the 24 h, the groups F, J, and M showed higher antimicrobial activity with statistically similar results, and presented intermediate performance, followed by I with the highest bacterial growth.

With respect to the time, it can be seen that with the exception of E group which grew within 24 h, all groups showed a statistically significant decrease in the bacterial growth.

**Table 6** Data in log<sub>10</sub> direct contact test of surface coating treatments suspensions with *C. albicans*, *S. aureus*, and *E. coli* after contact time of 1 h and 24 h

Surface coating treatments	<i>C. albicans</i>		<i>S. aureus</i>		<i>E. coli</i>	
	1 h	24 h	1 h	24 h	1 h	24 h
E	8.23 ± 0.05 A <sup>c</sup>	8.05 ± 0.07 B <sup>a</sup>	7.57 ± 0.10 A <sup>a</sup>	8.23 ± 0.07 B <sup>b</sup>	7.63 ± 0.11 A <sup>a</sup>	8.01 ± 0.11 B <sup>b</sup>
F	7.92 ± 0.07 A <sup>cd</sup>	8.08 ± 0.013 B <sup>b</sup>	7.69 ± 0.18 A <sup>b</sup>	7.920.07 B <sup>a</sup>	8.29 ± 0.05 A <sup>b</sup>	7.92 ± 0.07 B <sup>a</sup>
J	7.88 ± 0.11 A <sup>bd</sup>	8.15 ± 0.05 B <sup>b</sup>	7.95 ± 0.05 A <sup>b</sup>	7.88 ± 0.11 A <sup>a</sup>	8.38 ± 0.07 A <sup>c</sup>	7.88 ± 0.11 B <sup>a</sup>
I	7.64 ± 0.23 A <sup>b</sup>	8.26 ± 0.05 B <sup>d</sup>	7.69 ± 0.14 A <sup>b</sup>	8.30 ± 0.14 B <sup>b</sup>	8.35 ± 0.07 <sup>c</sup>	8.18 ± 0.10 A <sup>c</sup>
H	7.61 ± 0.11 A <sup>a</sup>	8.19 ± 0.03 B <sup>c</sup>	7.71 ± 0.14 A <sup>b</sup>	7.89 ± 0.16 A <sup>a</sup>	8.3 ± 0.06 A <sup>b</sup>	7.85 ± 0.09 B <sup>a</sup>

Different case letters in the same column represent a statistically significant difference among the groups at same exposure time ( $P < 0.05$ ). Different capital letters indicate the differences of each group at both different exposure times (1 and 24 h) ( $P < 0.05$ )

Different superscript letters represent statistically significant differences between groups and exposure times

**Codes:** **E:** PDMS film by casting and homogeneous method with 50% wt GO and 50% wt TiO<sub>2</sub> prepared by MAH method; **F:** PDMS film by casting and homogeneous method with 75% wt GO and 25% wt TiO<sub>2</sub> prepared by MAH method; **G:** PDMS film by casting and homogeneous method with 25% wt GO and 75% wt TiO<sub>2</sub> P25; and **H:** PDMS film by casting and homogeneous method with 100% wt GO

## Conclusions

An evaluation of the antibacterial activity on the surfaces of polymer nanocomposites PDMS/GO/TiO<sub>2</sub> was proposed. Two methods of incorporating TiO<sub>2</sub> particles and GO were analyzed, and the TiO<sub>2</sub> particles produced by MHA method and the commercial TiO<sub>2</sub> P25. Structural analysis ensured significant and promissory antimicrobial properties PDMS matrix as a function of the TiO<sub>2</sub> particles by MAH method in the interaction with the GO particle. The most effective films are the ones prepared by one step, which indicates the interactions of the particles with the polymer.

By analyzing the antimicrobial activity, the polymer embedded with GO and hydrothermal TiO<sub>2</sub> showed improved results against the bacteria and the fungus analyzed. These nanocomposites were shown to be functional and can be potentially applicable in coating surfaces, such as; medicinal packaging, hospital equipment, food and non-food coatings, and packaging industries.

**Acknowledgements** The authors are grateful to the Brazilian National Council for Scientific and Technological Development for financial support through CNPq (# 482251/2013-1), CNPq (#402127/2013-7), FAPERGS and CAPES.

## References

1. Carmeli Y (2008) Strategies for managing today's Infections. *J Compil Eur Soc Clin Microbiol Infect Dis* 14(Suppl. 3):22–31. doi:[10.1111/j.1469-0691.2008.01957.x](https://doi.org/10.1111/j.1469-0691.2008.01957.x)
2. Tran N et al (2015) Silver doped titanium oxide–PDMS hybrid coating inhibits *Staphylococcus aureus* and *Staphylococcus epidermidis* growth on PEEK. *Mater Sci Eng, C* 49:201–209. doi:[10.1016/j.msec.2014.12.072](https://doi.org/10.1016/j.msec.2014.12.072)
3. Zhang Q, Liu H, Chen X, Zhan X, Che F (2015) Preparation, surface properties, and antibacterial activity of a poly(dimethyl siloxane) network containing a quaternary ammonium salt side chain J. *Appl Polym Sci* 132, 41725 (1–8). doi:[10.1002/APP.41725](https://doi.org/10.1002/APP.41725)
4. Sankar GG, Sathya S, Murthy SP, Das A, Pandiyan R, Venugopalan VP, Doble M (2015) Polydimethyl siloxane nanocomposites: their antifouling efficacy in vitro and in marine conditions. *G Int Biodeterior Biodegrad* 104:307–314. doi:[10.1016/j.ibiod.2015.05.022](https://doi.org/10.1016/j.ibiod.2015.05.022)
5. Zhang G et al (2015) Enhanced flux of polydimethylsiloxane membrane for ethanol permselective pervaporation via incorporation of MIL-53 particles. *J Membr Sci* 492:322–330. doi:[10.1016/j.memsci.2015.05.070](https://doi.org/10.1016/j.memsci.2015.05.070)
6. Dumitriu C, Popescu M, Ungureanu C, Pirvu C (2015) Antibacterial efficiencies of TiO<sub>2</sub> nanostructured layers prepared in organic viscous electrolytes. *Appl Surf Sci* 341:157–165. doi:[10.1016/j.apsusc.2015.02.183](https://doi.org/10.1016/j.apsusc.2015.02.183)
7. Low W, Boonamnuayvitaya V (2013) Enhancing the photocatalytic activity of TiO<sub>2</sub> co-doping of graphene–Fe<sup>3+</sup> ions for formaldehyde removal. *J Environ Manage* 127:142–149. doi:[10.1016/j.jenvman.2013.04.029](https://doi.org/10.1016/j.jenvman.2013.04.029)
8. Hummers WS, Offeman RE (1958) Preparation of graphitic oxide. *J Am Chem Soc* 80(6):1339. doi:[10.1021/ja01539a017](https://doi.org/10.1021/ja01539a017)
9. Wang HE et al (2011) Rapid microwave synthesis of porous TiO<sub>2</sub> spheres and their applications in dye-sensitized solar cells. *J Phys Chem C* 115(21):10419–10425. doi:[10.1021/jp2011588](https://doi.org/10.1021/jp2011588)
10. Zhang H et al (2009) Antibacterial activity of endodontic sealers by modified direct contact test against *Enterococcus faecalis*. *J Endod* 35(7):1051–1055. doi:[10.1016/j.joen.2009.04.022](https://doi.org/10.1016/j.joen.2009.04.022)
11. Tian Y, Cai X, Wazir R, Wang K, Li H (2016) Water consumption and urinary tract infections: an in vitro study. *Int Urol Nephrol* 1:1–6. doi:[10.1007/s11255-016-1262-7](https://doi.org/10.1007/s11255-016-1262-7)

12. Yılmaz N, Ağuş N, Bayram A, Şamloğlu P, Şirin M, Derici Y, Hancı Y (2016) Antimicrobial susceptibilities of *Escherichia coli* isolates as agents of community-acquired urinary tract infection. *Turk J Urol.* 42(1):32–36. doi:[10.5152/tud.2016.90836](https://doi.org/10.5152/tud.2016.90836)
13. Puah M, Chua H, Tan J (2016) Virulence factors and antibiotic susceptibility of *Staphylococcus aureus* isolates in ready-to-eat foods: detection of *S. aureus* contamination and a high prevalence of virulence genes. *Int J Environ Res Public Health* 13(2):199. doi:[10.3390/ijerph13020199](https://doi.org/10.3390/ijerph13020199)
14. Martínez-Orozco RD, Rosu HC, Lee S-W, Rodríguez-González V (2013) Understanding the adsorptive and photoactivity properties of Ag-graphene oxide nanocomposites. *J Hazard Mater* 263:52–60. doi:[10.1016/j.jhazmat.2013.07.056](https://doi.org/10.1016/j.jhazmat.2013.07.056)
15. Wang C, Liua H, Liua Y, Heb G, Jiang C (2014) Comparative activity of TiO<sub>2</sub> microspheres and P25 powder for organic degradation: implicative importance of structural defects and organic adsorption. *Appl Surf Sci* 319:2–7. doi:[10.1016/j.apsusc.2014.05.014](https://doi.org/10.1016/j.apsusc.2014.05.014)
16. Hadavand BS, Ataefard M, Bafghi HF (2015) Preparation of modified nano ZnO/polyester/TGIC powder coating nanocomposite and evaluation of its antibacterial activity. *Compos B* 82:190–195. doi:[10.1016/j.compositesb.2015.08.024](https://doi.org/10.1016/j.compositesb.2015.08.024)
17. Ghassemia H, McGrath JE, Zawodzinski T Jr (2006) Sulfonated–fluorinated poly(arylene ether)s for a proton exchange membrane fuel cell. *Polymer* 47:4132–4139. doi:[10.1016/j.polymer.2006.02.038](https://doi.org/10.1016/j.polymer.2006.02.038)
18. Weiss EI, Shalhav M, Fuss Z (1996) Assessment of antibacterial activity of endodontic sealers by a direct contact test. *Endod Dent Traumatol* 12(4):179–184. doi:[10.1111/j.1600-9657.1996.tb00511.x](https://doi.org/10.1111/j.1600-9657.1996.tb00511.x)
19. Teymourpour S, Nafchi AM, Nahidi F (2015) Functional, thermal, and antimicrobial properties of soluble soybean polysaccharide biocomposites reinforced by nano TiO<sub>2</sub>. *Carbohydr Polym* 134:726–731. doi:[10.1016/j.carbpol.2015.08.073](https://doi.org/10.1016/j.carbpol.2015.08.073)
20. Li J, Wang G, Zhu H, Zhang M, Zheng X, Di Z, Liu X, Wang X (2014) Antibacterial activity of large-area monolayer graphene film manipulated by charge transfer. *Sci Rep* 4:4359. doi:[10.1038/srep04359](https://doi.org/10.1038/srep04359)